Clinical 3D and 4D Imaging of the Thoracic Aorta

D. Fleischmann[1], D.C. Miller[2]

[1] Department of Radiology, Stanford University Medical Center, Stanford

[2] Department of Cardiothoracic Surgery, Stanford University Medical Center, Stanford, CA, USA

Introduction

Modern day CT angiography (CTA) has replaced diagnostic angiography for the evaluation of thoracic aortic diseases. The development of CTA with retrospective ECG gating has been driven by coronary artery CTA, but it also provides significant benefits to imaging of the thoracic aorta. Retrospective ECG gating virtually eliminates cardiac pulsation artifacts and has therefore extended the clinical applicability of CTA to finally also include the aortic root. Moreover, ECG gating allows cardiac phase-resolved ('time-resolved') cine imaging and visualization, adding a 'fourth dimension' (4D) to this technique.

The first immediate clinical benefit of motion-free 3D imaging of the thoracic aorta is improved visualization and thus characterization of acute aortic dissection and its variants. In addition to the ability to visualize a dissection flap all the way to the aortic root and into the coronary arteries, it has become possible to precisely localize the site of intimal tears, which is increasingly important in the stent-graft era. Furthermore, motion-free images allow the detection of less-common, subtle but clinically equally important intimal lesions, which have been notoriously difficult to detect in vivo with any imaging modality [1]. We therefore use ECG gating routinely at our institution in all patients with acute aortic syndromes. The second clinical scenario in which ECG-gated thoracic CTA plays a central role, and thus has become a routine application at our institution as well, is in pre- and postoperative 3D and 4D imaging of patients with aortic-root diseases.

The purpose of this article is to explain the techniques of image acquisition as well as 3D and 4D visualization of the thoracic aorta using ECG-gated CTA. The clinical topics of this review focus on the practical application of this technique in the setting of acute aortic dissection with its variants, and on surgical treatment planning of patients with aneurysms of the aortic root.

CT Imaging Technique

A summary of the CT scanning and reconstruction parameters used with a 16-channel GE Lightspeed scanner and a 64-channel Siemens Sensation scanner are provided in Tables 1 and 2). A gated chest CTA is usually preceded by a non-enhanced CT series. Non-enhanced images are critical for the identification of intramural hematomas in the acute setting, and are indispensable for the identification surgical graft material and the differentiation of calcifications, Teflon pledgets, or glue from small leaks. CT scanning of nearly the entire thorax with retrospective ECG gating can be obtained with all 16- or more channel CT systems. The scanning range includes the origins of the supra-arch vessels down to the base of the heart. With 16-channel systems it is not possible to use the thinnest available collimation (e.g. 0.625, as would be used for a coronary CTA). A nominal section thickness of 1.25 mm is certainly adequate for visualization of the thoracic aorta, the aortic valve, and the course and origin of the coronary arteries. This protocol is not sufficient to rule out coronary artery stenoses, however. With 64-channel CT, we use a reconstructed section thickness of 1 mm for our gated chest protocol, and no premedication unless visualization of the coronary arteries is specifically requested. In the latter situation, we administer oral beta-blockers and sublingual nitroglycerin according to our coronary CTA protocol, but we use the larger scanning range (and longer scan time) for the entire chest. Except for obese patients (a tube output limited to 700 eff. mAs results in greater image noise), this protocol is technically and clinically equivalent to a coronary CTA (850 eff. mAs) and thus allows significant coronary artery disease to be ruled out.

Other than in coronary CTA, in which the reconstruction of one or very few datasets (e.g., a diastolic dataset at 65% of the RR-interval) suffices, gated chest studies require the reconstruction of several phases through the cardiac cycle. We generally reconstruct images through the entire chest at 65% of the RR-interval, and then reconstruct ten phases (from 0% through 90% of the RR-interval) of the heart and relevant portion of the thoracic aorta. These ten datasets can then be viewed as a cine-loop. In order to maintain similar image noise throughout the cardiac cycle, ECG dose modulation is not used in our gated chest protocol.

Good arterial opacification is a key element of CTA in general, and even more so if small structures, such as the aortic valve leaflets or tiny aortic-wall irregularities, are of diagnostic interest. We use high-concentration contrast medium (350-370 mg/ml) for all CT angiograms. For a 16-channel gated chest, we generally inject 5 ml/s (4.5-

Table 1. Scanning and injection parameters for retrospectively EKG-gated computed tomography angiography (CTA) of the thorax

	16-channel CT (GE LightSpeed 16)	64-channel CT (Siemens Sensation 64)
Premedication	none	None,or betablockers and sublingual nitroglycerine[a]
Pre-contrast series	Contiguous 2.5 mm	Contiguous 3 mm
Scanning range/direction	Above the aortic arch to the hiatus of diaphragm, cradio-caudal	
Tube voltage/current	120 kV/400 mA	120 kV/700 eff. mAs
Detector configuration	16×1.25mm	2×32×0.6-mm
Section thickness/reconstruction interval	1.25/0.8	1.0/0.7 0.75/0.5 mm[a]
Reconstruction phases	65% of RR-interval (entire scanning range), 0-90% of RR-interval (10 phases) of ascending aorta and heart (depending on the pathology)	
Scan time	~20-25 s	
Contrast medium	High-concentration (≥350 mg I/ml)	
Injection parameters	5 ml/s injection for duration of scan + 8 s (typically, 140 ml)	Biphasic injection, body-weight-based (see below)
Scanning delay	Minimum delay (automated bolus triggering, region of interest in ascending aorta)	

[a] If performed as a coronary CTA at the same time, the same premedication and thin-section thickness can be used with 64-channel systems

Table 2. Scanning and injection parameters for retrospectively EKG-gated CTA of the thorax with non-gated CTA of the abdomen and pelvis. All other acquisition and reconstruction parameters are as in Table 1

Scanning range		Above the aortic arch to the diaphragm (gated chest portion, and from the diaphragm to the lesser trochanter (non-gated portion)	
Scan time		Total scan time: ~20 s (gated chest) + 5 s interscan-delay + ~10 s (abdomen)	
Contrast medium		Biphasic, body-weight-adjusted injection protocol	
Injection parameters		Phase I (5s) injection rate (volume):	Phase II (total scan time of 5 s) injection rate;
	<55 kg	4.0 ml/s (20 ml)	3.2 ml/s (×scan time-5s)
	<65 kg	4.5 ml/s (23 ml)	3.6 ml/s (×scan time-5s)
Average	~75 kg	5.0 ml/s (25 ml)	4.0 ml/s (×scan time-5s)
	>85 kg	5.5 ml/s (28 ml)	4.4 ml/s (×scan time-5s)
	>95 kg	6.0 ml/s (30 ml)	4.8 ml/s (×scan time-5s)

6ml/s) for the duration of the scan time +8 s (e.g., for a 20-s scan we inject for 28 s, resulting in a total of 140 ml) (Table 1). The 8-s safety cushion compensates for the delay between the arrival of contrast medium in the ascending aorta and the initiation of the CTA acquisition above the aortic arch, inherent in the use of automated bolus triggering. For 64-channel gated chest studies and for all gated chest + abdomen and pelvis CTAs, we prefer biphasic injections. Biphasic injections with a short first high-flow-rate injection, followed by a second lower flow-rate maintenance injection provide bright vessel opacification at moderate total volumes of contrast for these relatively long scan times [2]. It is particularly important to set the total injection duration equal to the total-scan time, which also takes into account the (scanner-specific) 'interscan' delay between the gated portion (through the chest) and the non-gated CTA sequence through the abdomen and pelvis (Table 2). If this is ignored, abdominal and pelvic arterial opacification can be suboptimal or even inadequate for planning endovascular access.

3D and 4D Visualization

Powerful visualization tools are needed to take full advantage of the high-resolution multi-phase volumetric datasets (after first sentence in '3D and 4D Visualization' section): We use the AquariusNET server and thin client application (TeraRecon, Inc, San Mateo, CA) which allows to manage up to 28,000 CT slices simultaneously. While axial source images are always reviewed and remain the basis for diagnosis, real-time rendering and interaction with all ten phases of the cardiac cycle is key to analyzing aortic-root morphology and function. The possibility of cine viewing (looping through the datasets reconstructed at different RR-intervals) allows the selection of the best phase for a given abnormality. Moreover, cine-viewing provides invaluable dynamic information that is not obvious on static images from the systolic or diastolic phases only. Examples are small puffs of contrast-medium indicating the site of a small intimal tear or leak, and

motion abnormalities and functional deformities of the valve leaflets.

In addition to real-time interactive 2D, 3D and 4D (cine 3D) viewing of the datasets during image interpretation, it is important to also establish a consistent protocol of 2D, 3D, and 4D documentation for communicating the findings to the physicians involved in the patient's care. A typical set of images and movie clips of the thoracic aorta and the aortic root in a patient before surgical repair of a thoracic aortic aneurysm is provided in Fig. 1.

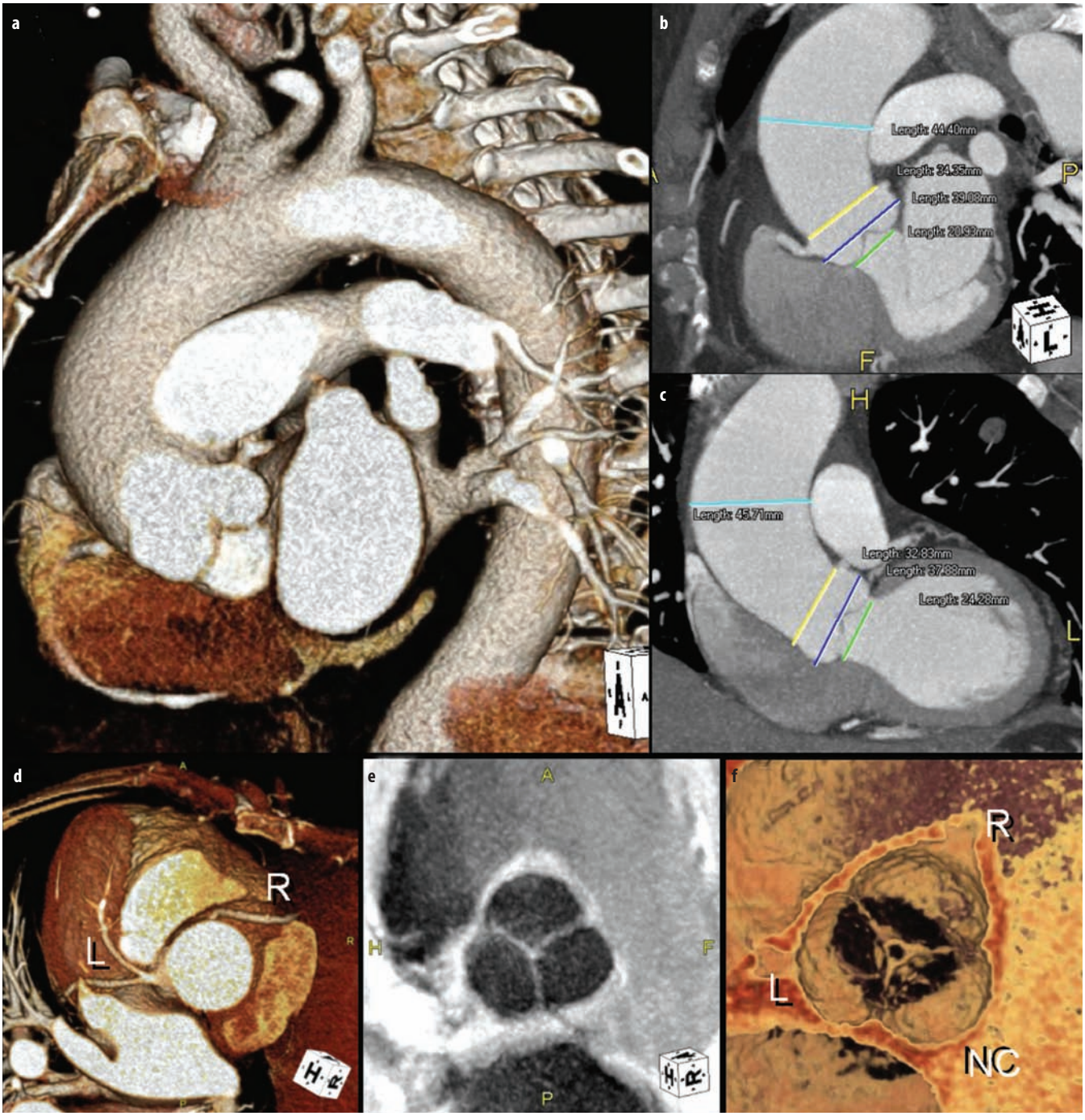

Fig. 1 a-f. Visualization of the thoracic aorta and the aortic root. Preoperative ECG-gated computed tomography angiography (CTA) of the chest in a 73-year-old woman with thoracic aortic aneurysm (64-channel CT, 0.75-mm section thickness, premedication with oral beta-blocker and sublingual nitroglycerine). (**a**) Volume-rendered view shows the ascending aortic aneurysm and generous aortic root. Measurements were obtained in oblique coronal and LAO views centered at the aortic valve (**b**, **c**) *Green* Anulus, *blue* sinuses of Valsalva, *yellow* sinotubular junction, *light blue* mid ascending aorta (**b**, **c**). Normal coronary anatomy is shown in (**d**). The aortic valve is visualized 'from above' using MinIP (**e**) and volume-rendered (**f**) images and movie clips. Note the small central valvular coaptation defect in (**f**), consistent with mild aortic regurgitation. Coronary arteries and/or sinuses of Valsalva are annotated as left (*L*), right (*R*), or non-coronary (*NC*)

An overview of commonly used rendering parameters employed at our institution is provided in Table 3.

Basic 2D multiplanar reformations (MPR) are commonly viewed in sagittal, coronal, or arbitrarily oblique cross-sections to make an initial diagnosis. We use 3D volume rendering (VR), maximum intensity projections (MIPs), and minimum intensity projections (MinIPs) to further interrogate the data. Typically, a slab of variable thickness is navigated through the dataset interactively, quite similar to the way a patient's body would be interrogated with an ultrasound probe. Familiarity with the principles of VR and a basic understanding of opacity transfer function settings is helpful to adjust parameters. For example, rendering the vessel lumen transparent (in order to visualize the aortic valve) usually requires adjusting the parameters to the degree of vessel opacification and image noise. This is straightforward with an intuitive user interface and preset templates. Thin (1-4 mm) MinIP slabs are ideally suited for visualizing low-attenuation structures (valve leaflets, tendinous chords) within high-attenuation surroundings (contrast-medium-opacified blood). Increasing the MinIP slab thickness makes very thin valves more visible in a noisy environment, but at the same time increases the thickness of the leaflets. Routinely inverting the gray scale of MinIP (Fig. 1e) images clearly identifies them as such, and thus distinguishes MinIPs from MIPs. MinIPs should not be used to visualize calcified valves.

The selection of rendering techniques, thickness, and orientation of the interrogating slab depends on the pathology at hand. In the acute setting, axial images alone are usually sufficient to make the diagnosis. Two-dimensional MPRs and 3D (or 4D) views are only generated if necessary to convey a particularly relevant finding, such as the location of an intimal tear relative to the supra-arch vessels before stent grafting. On the other end of the spectrum are elaborate, fairly standardized images, movie clips and measurements before surgical aortic-root reconstruction.

Surgical Anatomy of the Thoracic Aorta

The thoracic aorta begins at the ventriculo-aortic junction (often, but not semantically correctly referred to as the aortic anulus) and extends to the level of diaphragmatic hiatus, where it becomes the abdominal aorta. Diseases of the thoracic aorta - notably aortic dissection - commonly extend into the abdominal aorta and its branches. Therefore, imaging of the thoracic aorta requires that the chest, abdomen, and pelvic vasculature are imaged in their entirety. From a surgical perspective, the thoracic aorta is divided into four anatomic segments (Fig. 2): the aortic root, the ascending aorta (tubular portion), the transverse aorta (aortic arch), and the descending thoracic aorta.

– The *aortic root* consists of the *aortic anulus*, the *sinuses of Valsalva*, and the *sinotubular junction* (or ridge). The aortic anulus (Latin: small ring) at the site where the cusp hinges insert is not a planar anatomic structure since the ventriculo-arterial junction is not ring; rather,

Table 3. Post-processing techniques and parameters for preoperative visualization of the thoracic aorta

	Rendering technique and parameters	Views/images
Chest wall, 3D	VR, full-volume or slab; adjust transfer function to visualize bony and cartilaginous portions of the ribs	In patients with scoliosis and pectus excavatum (Marfan's), and in all re-do procedures, to show position of heart and vessels, notably the right coronary artery, relative to the sternum
Aorta, 3D overview[a]	VR, 5- to 8-cm thick slab, CTA-transfer function (opaque vessels)	'Candy cane' view; usually a LAO projection; shows which segments are involved as well as the position and orientation of the aorta in the chest
Aorta, diameters	Thin-slab MIPs (5 mm) Ascending Transverse Descending aorta MPR orthogonal	Thin-slab MIPs are obtained in LAO view; more than one image is required in very tortuous aortas. 'True' diameters should be obtained from MPR images oriented normal to the vessel axis if needed (e.g., stent-grafting)
Aortic root, 3D and 4D[b]	VR, 2- to 4-cm slab, transfer function adjusted to render vessel lumen transparent; adjustments needed to display calcifications as well Thin-slab MinIP (1-3 mm); inverted gray-scale Or thin slab MIP (1-3 mm) if calcified	View directed at the valve from above ('anesthesiologist perspective'). Provides 'inside' view of the 'hollow' sinuses, coronary origins, and aortic valve Capture systolic and diastolic views, as well as a cine-loop movie clips of aortic valve
Aortic-root, measurements[c]	MPRs or thin MIPs Anulus Sinuses of Valsalva Sinotubular junction	Oblique coronal and LAO (~3-chamber) views, with plane through center of valve, orthonormal measurements (e.g., at sinuses of Valsalva level)

VR, Volume rendering; *MIP*, maximum intensity projection; *MinIP*, minimum intensity projection; *MPR*, multiplanar reformation
[a] See Fig. 1a
[b] See Fig .1d-f
[c] See Fig. 1b, c

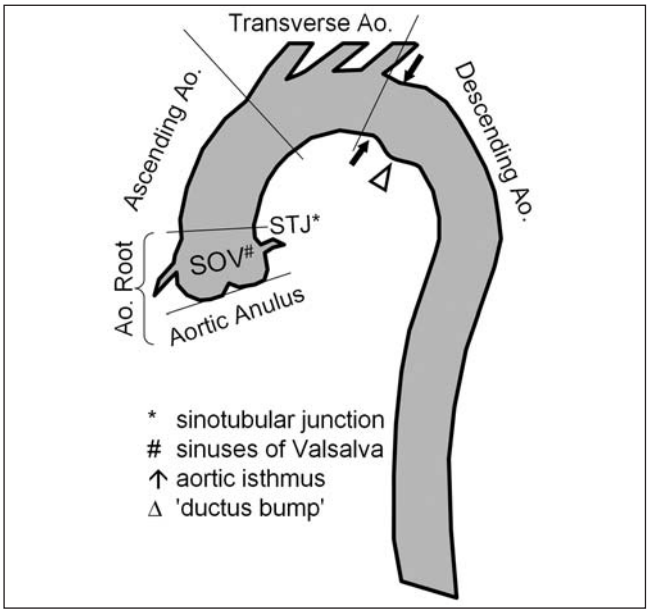

Fig. 2. Schematic view of the surgical anatomy of the thoracic aorta and the aortic root. *SOV* sinuses of Valsalva, *STJ* sinotubular junction, *arrow* aortic isthmus, *triangle* 'ductus bump'

it is a complex 'coronet' or crown-shaped three-dimensional structure. In between the three commissures are the subanular 'inter-leaflet triangles', one of which is the membranous septum. The normal anulus measures 27 mm in diameter or less, and is usually oval. The three sinuses of Valsalva (left, right, and non-coronary) contain the aortic valve with its three cusps. The left and right sinus of Valsalva give rise to the left and right coronary arteries, respectively. The highest points of the valve commissures/leaflet insertions are located at the level of the sinotubular junction, which is also the landmark separating the aortic root from the tubular portion of the ascending aorta.

- The *ascending aorta* refers to the aortic segments above the sinotubular ridge and proximal to the brachiocephalic artery.
- The *transverse aorta* or aortic arch is the segment containing the three supra-aortic branches; it begins proximal to the brachiocephalic artery and ends distal to the subclavian artery.
- The *descending thoracic* aorta begins distal to the left subclavian artery. The proximal portion of the descending aorta can be quite elongated, higher within the chest than the transverse aorta, and (misleadingly) assume the shape of an arch. Another anatomic feature of the normal descending thoracic aorta is a mild narrowing distal to the subclavian artery, the so called aortic neck or isthmus, and a smooth dilatation in the adjacent more distal portion of the aorta, anatomically referred to as the aortic spindle, but better known as the 'ductus bump.' The latter should not be confused with an aneurysm or a traumatic aortic transection.

The diameter of the normal thoracic aorta encompasses quite a wide, poorly defined range, and depends on the anatomic segment as well as the subject's age, sex, and body size [3]. In general, the aorta is larger proximally than distally. Men have larger aortic diameters than women. Aortic diameters increase throughout adult life with normal aging.

Aortic-Root Diseases

When the diameter of the aortic anulus exceeds 27 mm and the sinuses of Valsalva (SOV) are enlarged, the term 'anuloaortic ectasia' is used. For practical and imaging purposes, it is also sufficient to define a thoracic aortic aneurysm using a single diameter as a threshold. We use the term 'aneurysm' for any aortic segment (SOVs, sinotubular junction, ascending, transverse, and descending thoracic aorta) with a diameter >4 cm. The terms (mild/moderate) dilatation or ectasia are used for apparently wider segments that are ≤4 cm in diameter. Some patients, typically the elderly with long-standing hypertension, have diffuse aortic ectasia, in which the entire thoracic and abdominal aorta is moderately dilated.

Morphologically, thoracic aortic aneurysms can be described as saccular, fusiform, or diffuse. The most important descriptors, however, are the maximum diameter and the anatomic extent relative to the above-mentioned segments. An aortic-root aneurysm, ascending aneurysm, arch aneurysm, descending aneurysm, or any combination thereof each has its respective surgical implications.

The maximum diameter of a thoracic aortic aneurysm is an important predictor for the risk of dissection or rupture. In asymptomatic patients with Marfan syndrome or other congenital aortic diseases, surgical repair is indicated when the maximum aneurysm diameter reaches 5 cm (2.75 cm/m^2 body surface area) [4]. In patients with degenerative or atherosclerotic aneurysms, surgical repair is usually indicated when the maximum aneurysm diameter reaches 6-7 cm. Most thoracic aortic surgical authorities today use a '2×' rule, in which the diameter of a contiguous normal aortic segment is the denominator and the maximal aortic size is the numerator. If this ratio exceeds 2, surgical (or stent-graft) consideration is warranted as the risks of operation usually are less than the risk of aortic catastrophe within the next year. The ratio normalizes the dilated segment to the patient's normal aortic size and is valid in petite women as well as large men. In patients with Marfan syndrome and a positive family history of aortic catastrophe who are treated in centers with a documented clinical track record of successful valve-sparing aortic-root replacement and an operative mortality risk <1%, prophylactic operation is indicated when the aortic root is even smaller than the 2× the size of the normal distal ascending aorta, e.g., as small as 3.5-4 cm [5]. Other methods include normalizing aortic size to BSA or using the area of the maximally dilated segment (cm^2) divided by the patient's height (in meters) (if >10 cm^2/m, then operation should be con-

sidered). The indication for elective surgical repair of aortic-root aneurysms is usually determined by the presence and degree of aortic-valve incompetence due to stretching and subsequent non-coaptation of the valve cusps [6]. It should also be noted that the term 'sinus of Valsalva aneurysm' applies to aneurysms of a single sinus, rather than a dilatation of all sinuses (which should be described as root aneurysm) [7].

The etiology of aortic-root aneurysms is dominated by congenital, often inherited disorders and syndromes. The great majority of patients undergoing aortic-root replacement have either Marfan syndrome or bicuspid aortic valve (BAV) associated aneurysms. Other, less common heritable disorders are Ehlers Danlos (type IV) syndrome, and familial aortic aneurysm and dissection. While genetically diverse, all of these disorders result in strikingly similar pathologic features, traditionally (although misleadingly) referred to as 'cystic medial necrosis'; that is, elastolysis (degeneration and fragmentation of elastic fibers and collagen), mucoid degeneration (accumulation of basophilic ground substance in cell-depleted layer of the vessel wall; no cysts), smooth-muscle-cell loss and dedifferentiation (no necrosis). Similar degenerative changes can also be seen in normal aging and in patients with severe hypertension.

The aortic root can also be involved in degenerative atherosclerotic aneurysms of the ascending aorta. Other than in typical Marfanoid aortic-root aneurysms, in which the sinotubular junction is effaced resulting in the typical pear-shaped proximal aorta, the waist at the sinotubular junction is usually preserved in degenerative aneurysms of the ascending aorta. Involvement and dilatation of the sinotubular junction can nevertheless result in reduced cusp coaptation and aortic-valve incompetence (Fig. 1F). Other causes of aortic-root and ascending-aortic disease include infectious and inflammatory conditions, such as syphilis and giant cell (Takayasu) arteritis. Aortic dissection is discussed below.

Sinus of Valsalva aneurysms are also thought to be congenital in origin, caused by a developmental defect. This is supported by the frequent association with ventricular septal defects (30-60%), bicuspid aortic valve (~10%), and other congenital abnormalities. SOV aneurysms most commonly originate from the right sinus (65-85%), less commonly from the non-coronary sinus (10-30%), and rarely from the left sinus (<5%).

Marfan Syndrome

The incidence of Marfan syndrome is 1:3,00-1:5,000. This genetic disease can be inherited (autosomal dominant with variable penetrance) or occure as a spontaneous mutation of the fibrillin-1 gene [8]. The cardiovascular system (aortic aneurysm and dissection, mitral-valve prolapse), eye (ectopia lentis), and musculoskeletal system (dolichostemomelia, arachnodactyly, scoliosis, pectus deformity) are affected. Diagnosis is based on clinical criteria (Ghent nosology). Progressive aortic root dilatation leads to aneurysm and dissection, which are the leading causes of morbidity and mortality. Thoracic aortic dissection occurs in 40% of patients. Prophylactic aortic-root and ascending-aortic repair is indicated when the aortic diameter approaches 5 cm. Valve-sparing aortic-root replacement represents a reasonable alternative to composite valve-graft repair. Survival is excellent and complications are rare with either technique, but the long-term durability of valve-sparing aortic-root replacement has yet not been established (Fig. 3).

Bicuspid Aortic-Valve Disease

The incidence of bicuspid aortic-valve disease is very high, approximately 1:100 (4 million affected individuals in the USA). It has a 4:1 male predominance and familial aggregation. The disease is associated with coarctation of the aorta, patent ductus arteriosus, and coronary artery anomalies. While the most common fate is calcific aortic stenosis (85%), aortic-root enlargement, irrespective of altered hemodynamics, is highly prevalent (approx. 50%). Root enlargement is considered a precursor to aneurysm and dissection, and regular surveillance (echocardiography) is indicated [9]. Thoracic aortic dissection occurs in 5% of patients. Aneurysms involve the root as well as the ascending aorta, and typically extend into the (proximal) aortic arch (Fig. 4). Elective surgical repair is indicated when the aortic diameter approaches 5 cm, or when valvular complications occur. Valve-sparing aortic-root replacement is a reasonable alternative in patients whose valves are well-functioning.

Pre- and Postoperative CT Angiography of the Aortic Root

A basic understanding of surgical treatment options and techniques is helpful for diagnostic image interpretation, treatment planning, and particularly for post-operative follow-up. A detailed discussion of surgical techniques for treating aortic root and thoracic aortic diseases is beyond the scope of this article and can be found elsewhere [10]. Surgical access to the thoracic aorta is either from a median sternotomy (for the aortic root, ascending, and transverse aorta), or from a left lateral thoracotomy (arch and descending thoracic aorta). While a single tube-graft often suffices to replace the tubular portion of the ascending aorta, replacement or reconstruction of the aortic root is significantly more complex since the aortic valve and the coronary arteries have to be addressed. Several dedicated procedures using various graft/tissue materials have been derived over the years, i.e., composite valve graft and variants, valve-sparing procedures, homograft, pulmonary autograft (Ross procedure), stentless and bioprosthetic porcine root. Aortic-root replacement commonly requires the simultaneous replacement of parts or the entire ascending aorta, and may require partial (hemiarch) or complete replacement of the transverse aorta. Surgical replacement of the aortic arch is particu-

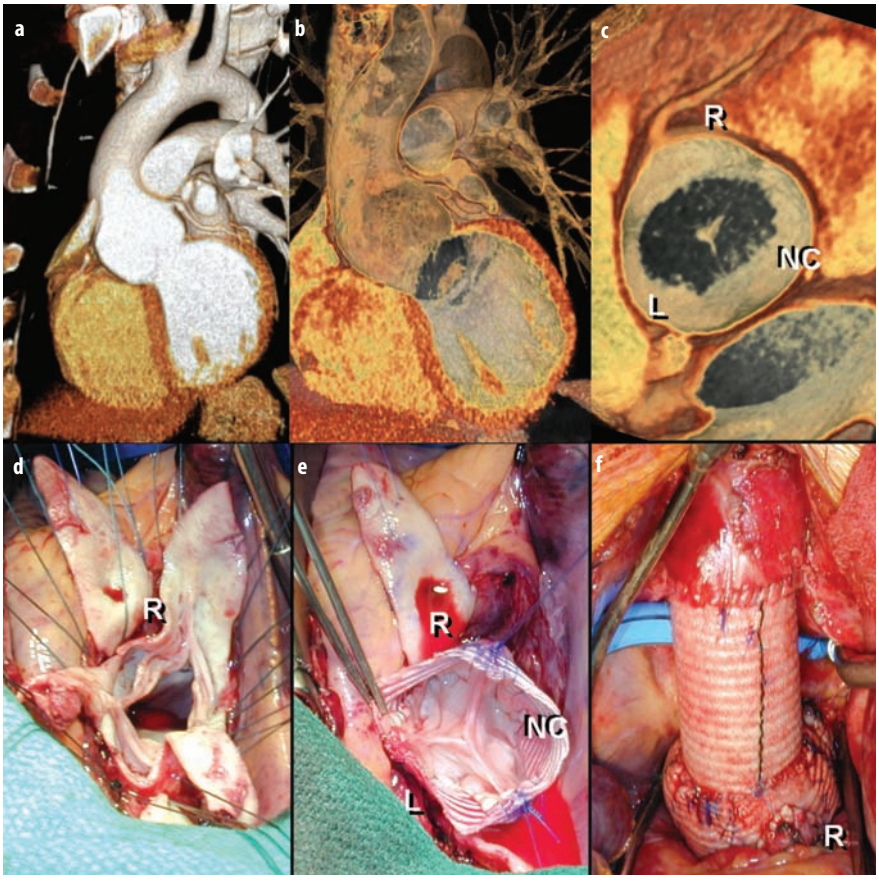

Fig. 3 a-f. Valve-sparing aortic-root replacement in a patient with Marfan syndrome. Preoperative volume-rendered image (**a**) of the thoracic aorta in a 27-year-old man with Marfan syndrome shows aneurysmal dilatation predominantly of the aortic root. Transparent-blood rendering (**b**) and a view 'from above the valve' (anesthesiologists perspective) (**c**) illustrate remarkable dilatation of the sinuses of Valsalva. Intraoperative photographs demonstrate (**d**) the flaccid aortic valve and the residual sinus tissue surrounding the valve commissures after resection of the sinuses of Valsalva. Note the sutures through the ventriculo-aortic junction, which is used to anchor the graft. The excised right coronary button (*R*) with the right coronary artery ostium is seen. (**e**) The aortic valve is seen resuspended within the proximal graft, which is anchored to the ventriculo-aortic junction (not shown). (**f**) An anterior view of the completed reconstruction of the aortic root with its neo-sinuses and the reimplanted right coronary artery (*R*), and the second tube graft replacing the tubular portion of the ascending aorta. Sinuses of Valsalva are annotated as left (*L*), right (*R*), or non-coronary (*NC*)

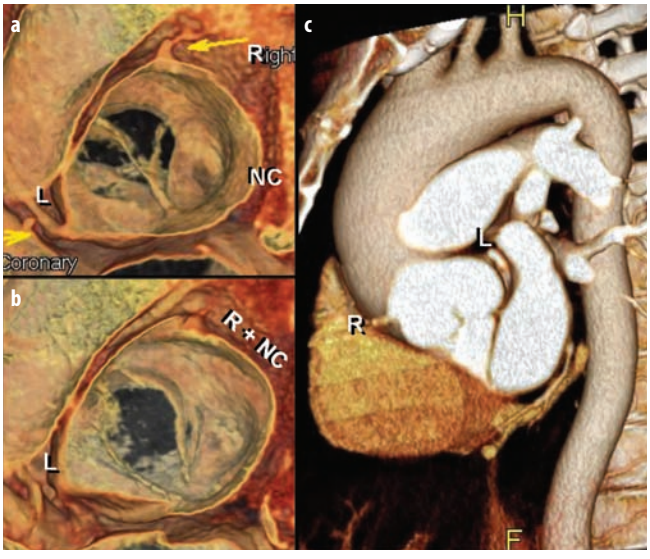

Fig. 4 a-c. Bicuspid aortic valve (BAV) disease. Volume-rendered diastolic (**a**) and systolic (**b**) images of the aortic root (transparent blood) in a 53-year-old woman show three sinuses of Valsalva (*R* right, *L* left, *NC* non-coronary) but two leaflets. In diastole (**a**), a raphé is seen between the right and non-coronary portions of the closed valve. In systole (**b**), however, the right and the non-coronary valve tissue are clearly fused (*R+NC*) to form a common valve leaflet. Note the typical shape of BAV-associated aneurysms, which involve the root, have their maximum diameters in the ascending aorta, and extend into the aortic arch. Compare with the normal descending aorta

larly challenging since reconstruction of the arch branches mandates hypothermic circulatory arrest and antegrade cerebral perfusion to protect the brain.

Aortic Root Replacement: Valve Sparing and Composite Valve Graft

Historically, the traditional surgical method of aortic-root replacement consists of a single graft that contains a mechanical valve - the so-called composite valve graft (CVG) [11]. In this procedure, the coronary artery ostia are reimplanted.

One increasingly popular alternative to CVG that avoids anticoagulation is valve-sparing aortic-root replacement. The basic idea is to replace the walls of the aortic root, while preserving the patient's own valve. Again, the coronary ostia need to be reimplanted. The various techniques of valve-sparing aortic-root replacement can be categorized into two broad groups [12]: (1) the Yacoub remodeling procedure, in which a scalloped graft is sewed to the residual portions of sinus tissue [13], and (2) the Tirone David reimplantation procedure, in which the proximal graft anastomosis is anchored at the ventriculo-aortic junction below the level of the cusps, and the valve commissures are then sewn inside the graft [14].

At our institution, a variant of the Tirone David [14] reimplantation technique (T. David-V, Stanford modifica-

tion) using two separate grafts has been the preferred approach since December 2002 [12]. The modified technique gives the surgeon unlimited flexibility to individualize the dimensions and 3D geometry of the root reconstruction according to the patient's specific pathoanatomy and creates 'neo-sinuses' in the vascular graft that mimic SOVs (Fig. 3).

Preoperative imaging and visualization with accurate measurements of the aortic anular and sinotubular junction diameter and cusp height help the surgeon to conceptualize the size of the graft, which is 'necked-down' (plicated) proximally to create the necessary anular size. Imaging also facilitates the determination of the appropriate diameter and height of the graft neo-sinuses and the size of the second graft above the neo-sinotubular junction.

Preoperative CT Angiography Image Evaluation

Image interpretation always includes a complete evaluation of the thorax by reviewing the transverse source images. The specific information sought in preoperative ECG-gated CTA of the thoracic aorta is listed below, and should be included in the radiological report. This information is supplemented by the respective 2D images, 3D images, and video clips (Table 3, Fig. 1):

- Type and size of aneurysm: Anatomic extent (e.g. aortic root aneurysm ± anuloaortic ectasia; ± involvement of ascending aorta; ± tapering into arch).
- Measurements: Diameters of anulus, SOVs, sinotubular junction, ascending, transverse and descending aorta.
- Aortic valve: Normal or abnormal; tricuspid vs. bicuspid. If bicuspid, describe morphology (one or two sinuses of Valsalva; which cusps are fused ± raphé); leaflet thickness, normal/abnormal motion (pliable or limited motion due to stretching of cusp edges), stenosis or incompetence [often caused by stretching of valve (central coaptation defect), or by valve prolapse (asymmetric coaptation defect)].
- Coronary-artery anatomy (and pathology): normal or abnormal coronary-artery anatomy. Note: variants can add significant complexity to surgery. Image-quality permitting (64-channel CT with modified coronary protocol), the presence/absence of coronary artery stenoses should be reported.

Other surgically relevant findings, such as the location/angle of the sternum relative to the mediastinal structures in patients with scoliosis or pectus excavatum, should also be included in the report. Attention should be given to postoperative changes from prior procedures (e.g., course of existing CABG grafts), if present.

Postoperative CT Angiography Image Evaluation

The first postoperative (pre-discharge) CT after aortic-root replacement is routinely obtained with retrospective ECG gating, in order to detect any early postoperative complications. Knowledge of the specific surgical procedure is often required to unambiguously interpret postoperative findings. Non-enhanced images are essential to identify graft material and may be the only clue as to what procedure was done when the (sometimes remote) surgical history is obscure. Post-operative image interpretation specifically attempts to:

- Identify grafts: On non-enhanced images, surgical grafts are slightly hyperdense. Also look for felt strips (reinforced anastomoses), felt pledgets (reinforced sutures), and BioGlue (after dissection repair), which should not be confused with small anastomotic leaks (on contrast-enhanced images).
- Detect potential pitfalls: Graft folds (at graft angles, or when the graft is plicated) or a so-called elephant trunk (free ending graft dangling in the descending aorta with its proximal anastomosis often in the region of the aortic neck and without a distal anastomosis) can simulate redissections. Tied-off graft cannulation sites, graft stumps (e.g., to the right axillary artery) or graft limbs (arch), which are used in cardiopulmonary bypass or cerebral perfusion (right axillary artery), can mimic small leaks or pseudoaneurysms. Unusual grafts (e.g., Cabrol aorto-coronary interposition graft) as well as unusual and 'historic' procedures (e.g., wrapping of the aortic wall around the graft, as in the original Bentall procedure) can be very difficult to interpret without the surgical history.
- Search for leaks and pseudoaneurysms: Proximal, distal, and graft to graft anastomoses, as well as coronary buttons should be evaluated. Small leaks (peri- supra- or infravalvular) may not be visible in all phases of the cardiac cycle! Review systolic and diastolic views! Pseudoaneurysms can also occur at arterial or cardiac cannulation sites.
- Rule out postoperative hematoma: Small amounts of retrosternal, pericardial, or periaortic fluid and stranding in the mediastinal fat are normal early postoperative findings. Consider adding a delayed phase (non-gated) CT acquisition to rule out small extravasations.
- Exclude infection: Graft infections and sternum osteomyelitis are rare but difficult to treat late complications. Imaging findings range from extensive abscess-like fluid collections with rim enhancement and contained ruptures, to small amounts of perigraft fluid collections. Minimal soft-tissue density abnormalities may harbor infected and necrotic tissue and further imaging (white cell scan) should be recommended in the proper clinical setting.

Acute Aortic Dissection Variants

Imaging plays a central role in the diagnostic evaluation and management of patients with acute conditions of the aorta - the so-called acute aortic syndromes (Table 4). Modern multidetector-row CT technology has become increasingly available in the 24/7 emergency setting, with sensitivity and specificity both approaching 100%

Table 4. Acute aortic syndromes

Dissection and variants
Classic dissection
Intramural hematoma
Limited intimal tear
Penetrating atherosclerotic ulcer
Intramural hematoma
Pseudoaneurysm/contained rupture
Rupturing aortic aneurysm

for the detection of acute aortic disorders, and with the ability to detect alternative findings [15]. With the advent and increasing use of endovascular stent-grafting [16, 17], CT has also assumed a critical role in treatment planning. Stent-grafting requires not only accurate 3D measurements and localization of the intimomedial flap, but also a clear depiction of the site of the intimal tear as the primary treatment target. Covering the culprit intimal tear in the descending aorta may be a viable treatment strategy even in patients with (retrograde) type A dissection.

We have found retrospective ECG-gating of the thoracic aorta to be very helpful in the characterization of aortic dissections, and we use this technique routinely in patients presenting with acute aortic syndromes. Near-motion-free images allow identification of the site of the intimal tear, the location of the intimomedial flap, and its motion, which can be delineated even when extending into the aortic root and coronary arteries. Another consequence of using increasingly powerful CT equipment in the evaluation of acute aortic diseases is the ability to see more subtle abnormalities and variants of aortic dissections, and their evolution over time, which may ultimately expand our understanding of these disorders.

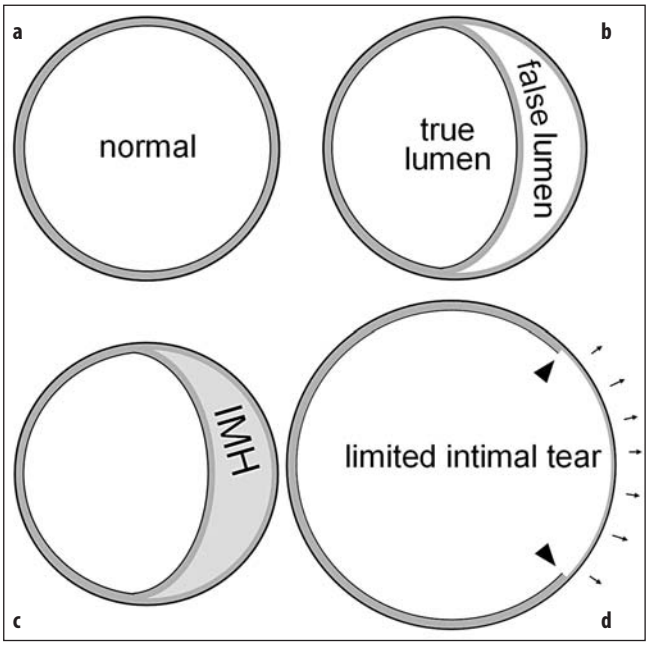

Fig. 5 a-d. Aortic dissection variants. (**a**) The layers of the normal aortic wall consist of the intima, the media, and the adventitia. Most of the substance of the aortic wall is media (*gray*). Neither the intima nor the adventitia (*black inner and outer contours* of the aortic wall) is visible on CT. All dissection variants have an abnormal media in common, historically referred to as 'cystic media necrosis' (see text for details). Classic aortic dissection (**b**) occurs within the outer third of the medial layer, resulting in two channels of blood flow. Note that the tissue separating the true and false lumen is mostly media tissue, and correctly should be termed the intimomedial flap (in lieu of intimal flap). (**c**) When the separation plane within the media is filled with stationary blood, instead of flowing blood, this is an intramural hematoma (*IMH*). A limited intimal tear (**d**) is a partial-thickness tear (*arrowheads*) through the intima and inner portion of the media, thus exposing the residual media/adventitia, which tends to bulge out (*small arrows*) relative to the remainder of the aortic circumference

Classic Aortic Dissection and Intramural Hematoma

Aortic dissection is an uncommon yet potentially catastrophic clinical event. The incidence has been estimated at 5-30/million/year (vs. 4,400/million/year for acute myocardial infarction in the USA). Acute aortic dissection is the most common acute aortic condition requiring urgent surgery. While the initiating event leading to aortic dissection is unknown, the common feature in most patients is a structural abnormality of the aortic media. Degeneration of the elastic fibers and smooth muscle cells of the aortic media is seen in patients with Marfan syndrome (and other heritable disorders leading to aortic aneurysms and dissections; see above) and in patients with hypertension. Intimal disease (atherosclerosis) is not a prerequisite for aortic dissections.

Classic aortic dissection is characterized by the presence of an entry tear in the intima and a clear separation between layers of the aortic media, resulting in two separate flow channels, i.e., the true lumen, and the false lumen (a channel entirely within the media) (Fig. 5). The relative flow of blood and the shape of the true and false lumens are highly variable and probably depend on the size of the entry tear, the degree of media degeneration, the presence, location, number, and size of re-entry tears (where false-lumen blood flow reenters or communicates with the true lumen). Neither the size of the channels nor the orientation and degree of arterial enhancement necessarily allow identification of the true and false lumen, respectively. However, modern CT technology provides reliable identification of the flow channels by analyzing the entire aorta and tracing the respective lumens. This is particularly important when ischemic complications occur (cerebral, renal, mesenteric, or lower limb).

Involvement of the ascending aorta in acute dissection is a surgical emergency owing to its high mortality if left untreated. Fluid seeping through the diseased wall can lead to pericardial tamponade. Ascending dissections can extend into the SOVs and into the coronary artery ostia,

causing valve incompetence, myocardial ischemia, and leading to frank rupture.

There is considerable overlap between intramural hematoma (IMH) and aortic dissection, in terms of underlying media degeneration, patient population, and risk of rupture. IMH is considered a variant of classic dissection, where the above mentioned layer within the aortic media is not filled with flowing, but with stationary blood (Figure 5). Presenting features are similar, progression to dissection may occur, and treatment considerations are similar to classic dissection [18].

Limited Intimal Tear (Limited Dissection)

So-called isolated or limited intimal tears are probably the least common and less well-known intimomedial lesions of the aorta. The true prevalence and spectrum of these lesions is unknown but, if specifically searched for, may be up to 5% of patients undergoing acute ascending aortic repair [1]. The clinical implications are identical to those of other acute aortic syndromes, and surgical repair is indicated in these cases, which usually affect the ascending aorta. Chronic limited tears have also been described, notably in patients with Marfan syndrome.

Owing to their morphology, these lesions are particularly difficult to detect on imaging studies. In fact, the nine patients described in Sevensson's original description were all diagnosed intraoperatively despite multiple preoperative noninvasive and invasive studies [1].

Pathologically these lesions represent partial-thickness linear or stellate tears through the intima and underlying superficial media, exposing the deeper media and adventitia [1]. The edges of the tear may show limited undermining but, oddly enough, this does not result in a more extensive separation between the torn and intact layers of the aortic wall, as one might expect. Intramural blood has not been described as a typical feature of this lesion, but we have observed both a tiny intimal flap and a small intramural hematoma at the two ends of a longitudinal tear in a patient imaged with ECG-gated CTA (Fig. 6). The edges of the tear are separated from each other, probably due to stretching of the residual aortic wall (consisting of remaining intact media and adventitia) or some elastic recoil of the torn layer, resulting in an eccentric bulge of the aorta. An eccentric bulge may be the only imaging sign of this significant lesion, and these lesions have been under-diagnosed with all imaging modalities (US, CT, MR). It is not clear what determines whether a classic dissection with a septum, intramural hematoma, or limited intimal tear occurs.

While it is reasonable to assume that the sensitivity of ECG-gated CTA will improve the detection of these subtle ascending aortic lesions, this has not been established. The main implication for the radiologist is therefore to be aware of the fact that these subtle lesions indeed exist and should be searched for with the appropriate technique and in the right clinical setting.

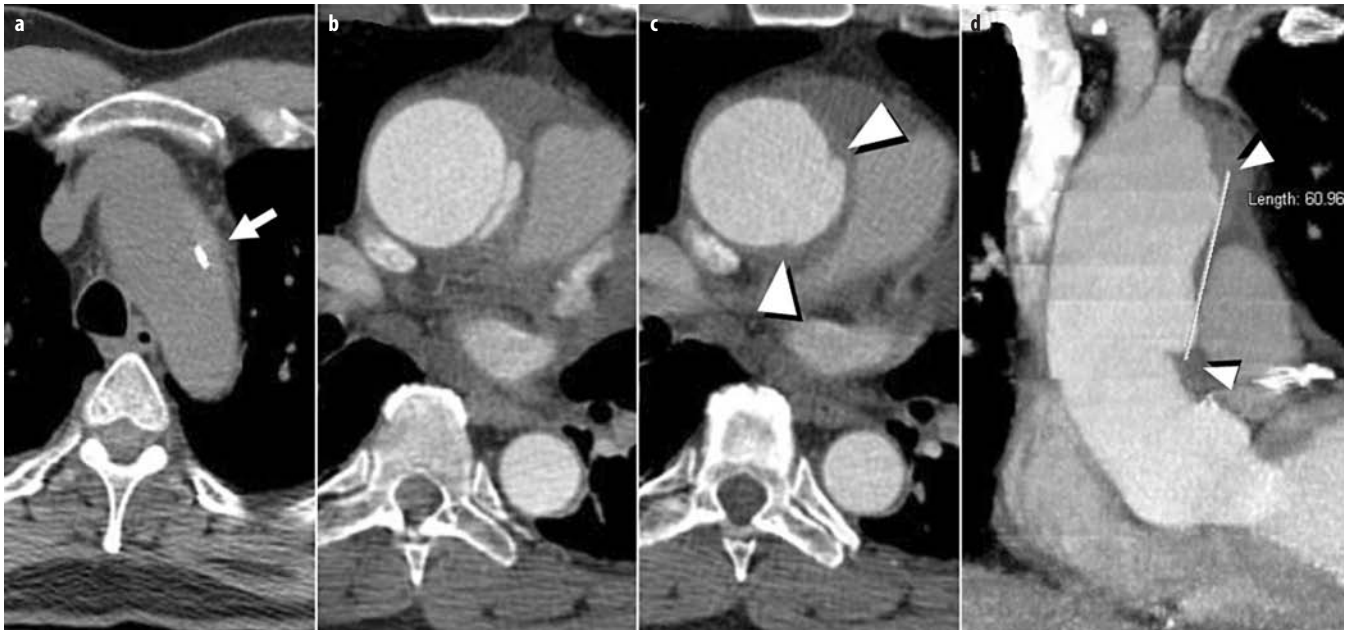

Fig. 6 a-d. Limited intimal tear of the ascending aorta. Non-enhanced CT image (**a**) and ECG-gated axial CTA images (**b**, **c**) show a small intramural hematoma at the level of the proximal aortic arch (*arrow* in **a**). Note the displaced small calcification, indicating the location of the intima. In the proximal ascending aorta, a single image (**b**) demonstrates a small flap, consistent with an undermined edge of a limited intimal tear. Image (**c**), immediately superior to (**b**), shows the edges of the limited intimal tear (*arrowheads*) and the bulge of the exposed residual aortic wall (*small arrows*). The full longitudinal extent of the lesion is shown in a thin-slab maximum intensity projection image (**d**): The tear extends from the proximal ascending aorta to the proximal arch, with a length >6 cm

Anatomic Classification of Aortic Dissection

We use the 1970 Stanford classification to describe the type of dissection and the extent of the intimal (intimomedial) flap [19]. In addition, we specifically describe the site of the primary intimal tear (PIT), as advocated by Griepp's Mt. Sinai cardiovascular surgical group [20], which was not included in the original Stanford classification scheme. The definition of a Stanford type A dissection is based on the presence of a dissection flap in the ascending aorta, whereas a Stanford type B dissection - irrespective of the location of the PIT [ascending, arch, descending (retro-A dissection), or abdominal aorta] - is defined by the absence of a dissection flap in the ascending aorta. Note that the definition of type A vs. type B is thus exclusively based on the involvement or not of the ascending aorta. This is clinically meaningful because it predicts the expected biological behavior of the process if untreated, and therefore dictates management; for example, ascending aortic involvement (acute type A dissection) mandates emergency surgical repair. While most type B dissections commonly involve the descending aorta distal to the subclavian artery and frequently the abdominal aorta, this is not how type B dissections are strictly defined (despite the notorious propagation of misinterpretation in the literature). Type B dissections also include those that involve the transverse aorta (aortic arch) due either to the PIT being located in the arch or to retrograde propagation of the false lumen back up into the arch. Regardless of arch involvement, most patients with acute type B dissections are treated conservatively unless complications, such as rupture, leak, distal body malperfusion due to true lumen collapse, rapid false lumen expansion, refractory pain, malignant hypertension, or branch-vessel ischemia, require urgent surgical or stent-graft intervention. The terms type A and type B are also used to describe the location of aortic intramural hematoma (IMH). More detailed anatomic descriptions of the location of IMH have recently been proposed in the literature [18].

Penetrating Atherosclerotic Ulcer

Penetrating atherosclerotic ulcers (PAUs) are a rather distinct entity within the acute aortic syndromes. Pathologically, these lesions are defined as ulcers of the inner lining of the aorta (usually, a thickened intima with chronic atherosclerotic change) that penetrate through the internal elastic lamina into the aortic media, which may result in a local aortic-wall hematoma. Alternatively, the ulcer may penetrate through the entire aortic wall and result in a (contained) rupture.

The radiologic diagnosis of a PAU is based on the presence of an ulcer-like aortic-wall lesion (the internal elastic lamina is not visible on imaging studies) that typically protrudes beyond the aortic circumference and is associated with a local intramural hematoma or signs of rupture. Clinical correlation is important, since ulcer-like lesions can be an incidental finding in asymptomatic patients, representing either an ulcerated plaque (not penetrating into the media) or a chronic, healed (reendothelialized) ulcer. There is a continuum between the latter lesions and atherosclerotic aneurysms.

Penetrating aortic ulcers can be considered a consequence of a diseased intima (i.e., atherosclerosis), in contradistinction to aortic dissection and its variants. In these latter entities, intimal disease is not a prerequisite, but degenerative changes of the elastic fibers and smooth muscle cells of the aortic media are the rule. This is also in keeping with the observation that in older patients with significant atherosclerotic plaques PAUs tend to occur in the descending thoracic aorta. More than one PAU is not uncommon in a given patient. The fact that both PAUs and the dissection-complex can result in the accumulation of blood in the aortic wall as an intramural hematoma may be considered a mere coincidence. The IMH seen in patients with PAUs are usually more focal than those seen in patients with IMH alone. If 'intimal flaps' are seen in patients with PAUs, these may be regarded as deep overhanging edges of an ulcer rather than true dissections. Nonetheless, some morphologic overlap and ambiguity on imaging studies does occur. The therapeutic consequences in the appropriate clinical setting are the same for any morphology, independent of the semantics.

CT Angiography Image Evaluation in Acute Aortic Syndromes

The diagnostic evaluation of patients with acute aortic syndromes is based on a thorough review of the transverse source images. Simple 2D reformations can be very helpful in the assessment of aortic dissections. ECG gating substantially improves the quality of images of the aortic root and ascending thoracic aorta. Three- and 4-dimensional visualization is helpful for treatment planning. The specific information sought in patients with acute aortic syndromes should comprise:

- Lesion characterization: Dissection and its variants vs. PAU. The presence of intramural hematoma and flow channels should be determined on non-enhanced images.
- Anatomic extent: The extent of the intimo-medial flap (Stanford Type A vs. Type B) the site of intimal tear should be described.
- True vs. false lumen and side-branch involvement: The entire aorta should be scrutinized in order to identify true and false lumens, notably in the presence of side-branch ischemia.
- Complications: Pericardial fluid and signs of rupture, e.g., periaortic hematoma and hemothorax should be noted. Mild periaortic stranding should be mentioned if present, but is not a definite sign of rupture in stable/asymptomatic patients. Signs of organ (kidneys, bowel) malperfusion should also be looked for.

– Stent-graft planning: Measurements of aortic diameters, distance of the intimal flap and tear from the subclavian and left carotid artery origins should be measured. Femoral and pelvic vessel size and tortuosity should be assessed for stent-graft planning.

References

1. Svensson LG, Labib SB, Eisenhauer AC, Butterly JR (1999) Intimal tear without hematoma: an important variant of aortic dissection that can elude current imaging techniques. Circulation 99:1331-1336
2. Fleischmann D, Rubin GD, Bankier AA, Hittmair K (2000) Improved uniformity of aortic enhancement with customized contrast medium injection protocols at CT angiography. Radiology 214:363-371
3. Roman MJ, Devereux RB, Kramer-Fox R, O'Loughlin J (1989) Two-dimensional echocardiographic aortic root dimensions in normal children and adults. Am J Cardiol 64:507-512
4. Davies RR, Gallo A, Coady MA et al (2006) Novel measurement of relative aortic size predicts rupture of thoracic aortic aneurysms. Ann Thorac Surg 81:169-177
5. Kim SY, Martin N, Hsia EC et al (2005) Management of aortic disease in Marfan syndrome: a decision analysis. Arch Intern Med 165:749-755
6. Bonow RO, Carabello BA, Kanu C et al (2006) ACC/AHA 2006 Guidelines for the management of patients with valvular heart disease: a report of the American College of Cardiology/American Heart Association Task Force on Practice Guidelines (writing committee to revise the 1998 Guidelines for the Management of Patients With Valvular Heart Disease): developed in collaboration with the Society of Cardiovascular Anesthesiologists: endorsed by the Society for Cardiovascular Angiography and Interventions and the Society of Thoracic Surgeons. Circulation 114:e84-e231
7. Ring WS (2000) Congenital Heart Surgery Nomenclature and Database Project: aortic aneurysm, sinus of valsalva aneurysm, and aortic dissection. The Annals of Thoracic Surgery 69:147-163
8. Judge DP, Dietz HC (2005) Marfan's syndrome. Lancet 366:1965-1976
9. Fedak PW, Verma S, David TE et al (2002) Clinical and pathophysiological implications of a bicuspid aortic valve. Circulation 106:900-904
10. Gardner TJ, Spray TL, Rob C (2004) Operative cardiac surgery. Arnold (distributed in the USA by Oxford University Press) London, New York
11. Bentall H, De Bono A (1968) A technique for complete replacement of the ascending aorta. Thorax 23:338-339
12. Miller DC (2003) Valve-sparing aortic root replacement in patients with the Marfan syndrome. J Thorac Cardiovasc Surg 125:773-778
13. Sarsam MA, Yacoub M (1993) Remodeling of the aortic valve anulus. J Thorac Cardiovasc Surg 105:435-438
14. David TE, Feindel CM (1992) An aortic valve-sparing operation for patients with aortic incompetence and aneurysm of the ascending aorta. J Thorac Cardiovasc Surg 103:617-621
15. Hayter RG, Rhea JT, Small A et al (2006) Suspected aortic dissection and other aortic disorders: multi-detector row CT in 373 cases in the emergency setting. Radiology 238:841-852
16. Dake MD, Kato N, Mitchell RS et al (1999) Endovascular stent-graft placement for the treatment of acute aortic dissection. N Engl J Med 340:1546-1552
17. Dake MD, Wang DS (2006) Will stent-graft repair emerge as treatment of choice for acute type B dissection? Semin Vasc Surg 19:40-47
18. Evangelista A, Mukherjee D, Mehta RH et al (2005) Acute intramural hematoma of the aorta: a mystery in evolution. Circulation 111:1063-1070
19. Daily PO, Trueblood HW, Stinson EB et al (1970) Management of acute aortic dissections. Ann Thorac Surg 10:237-247
20. Ergin MA, O'Connor J, Guinto R, Griepp RB (1982) Experience with profound hypothermia and circulatory arrest in the treatment of aneurysms of the aortic arch. Aortic arch replacement for acute arch dissections. Journal of thoracic and cardiovascular surgery 84:649-655